Journal of Geophysical Research: Earth Surface

RESEARCH ARTICLE
10.1029/2018JF004771

**Key Points:**
- Southern California beach response to the 2015–2016 El Niño varied widely, from considerable erosion to accretion
- Some coastal erosion and damage were limited by the timing of high tides and large waves, northerly swell direction, and low rainfall
- Estuary mouths on average accreted, while their adjacent beaches eroded. Many estuaries remained or became closed during the study

**Supporting Information:**
- Supporting Information S1
- Table S1

**Correspondence to:**
A. P. Young,
adyoung@ucsd.edu

**Citation:**
Young, A. P., Flick, R. E., Gallien, T. W., Giddings, S. N., Guza, R. T., Harvey, M., et al. (2018). Southern California coastal response to the 2015–2016 El Niño. *Journal of Geophysical Research: Earth Surface*, *123*, 3069–3083. https://doi.org/10.1029/2018JF004771

Received 31 MAY 2018
Accepted 31 OCT 2018
Accepted article online 5 NOV 2018
Published online 27 NOV 2018



# Southern California Coastal Response to the 2015–2016 El Niño

**Adam P. Young[1], Reinhard E. Flick[1], Timu W. Gallien[2], Sarah N. Giddings[1], R. T. Guza[1], M. Harvey[1], Luc Lenain[1], B. C. Ludka[1], W. Kendall Melville[1], and W. C. O'Reilly[1]**

[1]Scripps Institution of Oceanography, University of California San Diego, La Jolla, California, USA, [2]Civil and Environmental Engineering, University of California, Los Angeles, California, USA

**Abstract** Widespread erosion associated with energetic waves of the strong 2015–2016 El Niño on the U.S. West Coast has been reported widely. However, Southern California was often sheltered from the northerly approach direction of the offshore waves. The few large swells that reached Southern California were not synchronous with the highest tides. Although west coast-wide tidal anomalies were relatively large in 2015–2016, in Southern California, total water levels (sum of tides, anomalies, and wave superelevation) were lower than during the 1997–1998 Niño, and comparable to the 2009–2010 Niño. Airborne lidar surveys spanning 300 km of Southern California coast show the beach response varied from considerable erosion to accretion. On average, the shoreline moved landward 10 m, similar to the 2009–2010 El Niño. Some San Diego county beaches were narrower in the 1997–1998 El Niño than in 2015–2016, consistent with the higher erosion potential in 1997–1998. Beach retreat exceeded 80 m at a few locations. However, 27% of the shoreline accreted, often in pocket beaches, or near jetties. While adjacent beaches eroded, estuary mouths accreted slightly, and several estuaries remained or became closed during the study period. Only 12% of cliffs eroded (mostly at the base), and the average cliff face retreat was markedly less than historical values. Only two cliff-top areas retreated significantly. Although some areas experienced significant change, the potential for coastal erosion and damage in Southern California was reduced compared to the 1997–1998 El Niño, because of low rainfall, a northerly swell approach, and relatively limited total high-water levels.

## 1. Introduction

Transportation, critical infrastructure, military installations, public beaches and parks, and private development in Southern California have long been subject to flooding, erosion, and damage. With the added pressure of accelerated sea level rise and increases in extreme water level events (e.g., Tebaldi et al., 2012), the public, coastal policy-makers, and property owners will face ever more contentious and costly trade-offs between beach sand nourishment, armoring, and managed retreat. Beaches, cliffs, and estuaries form the primary natural components of the Southern California coastal system. Feedback couple these three elements to each other and the built environment.

As measured by the multivariate El Niño–Southern Oscillation (ENSO) index (Wolter & Timlin, 2011), the 2015–2016 El Niño was one of the three strongest El Niño–Southern Oscillation events in the last 65 years (Huang et al., 2016). Strong El Niños in California usually elevate winter precipitation, wave heights, and sea levels, causing increased coastal erosion, flooding, and damage (Barnard et al., 2011; Bromirski et al., 2003; Cayan et al., 2008; Flick, 1998; Sallenger et al., 2002; Storlazzi & Griggs, 2000; Strolazzi et al., 2000). Barnard et al. (2017) showed that the average shoreline retreat (change) in each of six U.S. West Coast regions during the 2015–2016 El Niño was the highest on record. Doria et al. (2016) showed that several Southern California beaches eroded farther landward during the 1997–1998 El Niño than the 2009–2010 El Niño. Ludka et al. (2016) showed that one Southern California beach eroded to a new low during the 2015–2016 El Niño (over a seven-year monitoring period), while three other recently nourished San Diego County beaches maintained widths above previous El Niño lows. Ludka et al. (2016), Doria et al. (2016), and Barnard et al. (2017) used the same ~20-km total alongshore span to evaluate the effects of the 2015–2016 El Niño on Southern California shorelines. Here airborne lidar spanning 300 km of Southern California coast shows significant alongshore variation in beach change. Additionally, cliff erosion and estuary mouth morphology during the 2015–2016 El Niño were measured. The results are compared with the last two large El Niño events, occurring in 1997–1998 and 2009–2010.

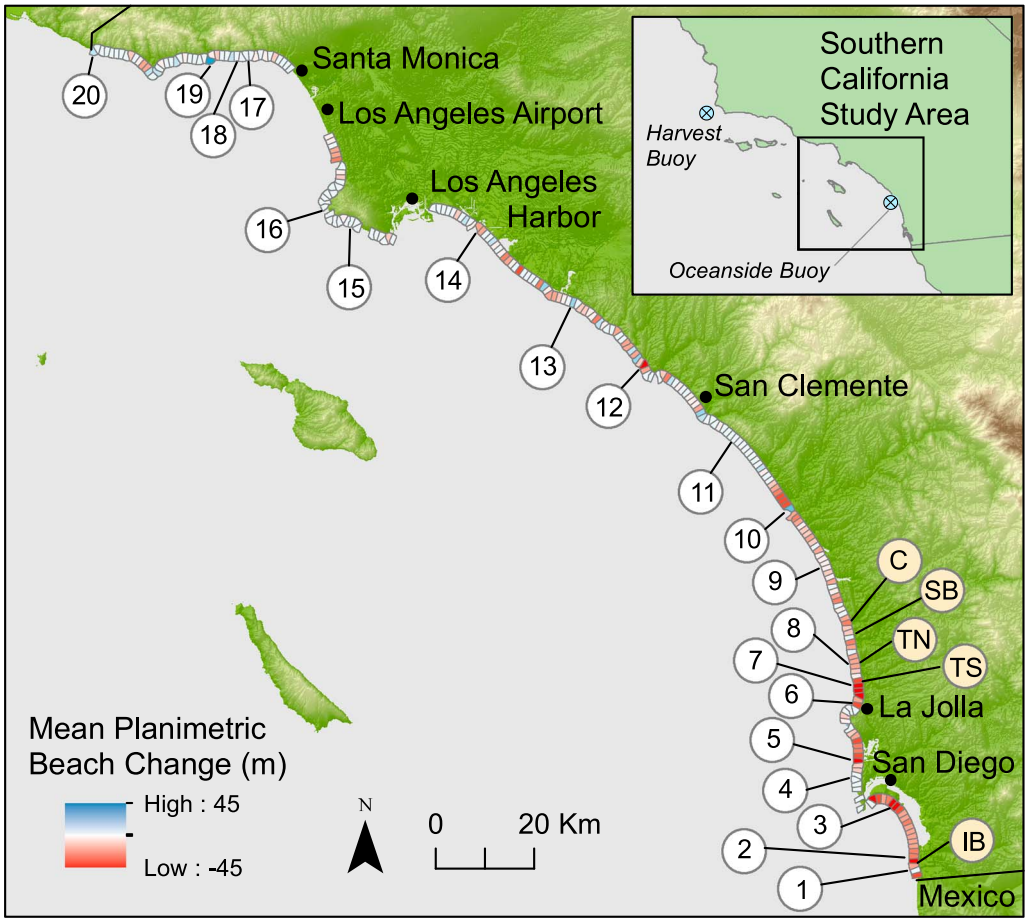


**Figure 1.** Study area map. Planimetric beach changes (6 October 2015 and 22 March 2016) are averaged over 1-km sections (see color bar). Notable coastal change and damage locations: (1) Tijuana inlet migrated; (2) Imperial Beach erosion and flooding; (3) Silver Strand berm overtopped; (4) Point Loma sea-arch collapse; (5) Dog Beach, Ocean Beach, beach retreat; (6) La Jolla Shores, beach erosion; (7) Blacks Beach, beach erosion; (8) Los Peñasquitos lagoon area, damage to roadside parking and access ramp and inlet closure; (9) Carlsbad, 600 m of continuous cliff base erosion (Figure S1a); (10) north side of Oceanside harbors, beach progradation; (11) San Onofre, large cliff failure; (12) Salt Creek pocket beach rotation, major beach erosion; (13) just north of Newport harbor, beach progradation; (14) just south of Seal Beach inlet jetty, beach erosion; (15) Portuguese bend landslide; (16) Christmas tree cove landslide; (17) new riprap seawall and slope reconstruction; (18) slope reconstruction; (19) Malibu Creek inlet, beach progradation; and (20) Leo Carillo parking lot erosion. Beaches with long-term monitoring: (IB) Imperial Beach, (TS) Torrey Pines south, (TN) Torrey Pines north, (SB) Solana Beach, and (C) Cardiff State Beach shown in Figure 6. Inset show Southern California study location and the Harvest and Oceanside buoy locations.

## 2. Southern California Study Region

The 300-km-long study area extends from the Los Angeles-Ventura County Line south to the international border (Figure 1). The coast primarily consists of beaches backed by lowlands, lagoons, and cliffs. Beaches are absent at jettied harbor mouths, headlands, and some rocky cliffs. Regional urbanization and development have significantly altered the coastline. Cliffs are typically 10–30 m high, but sometimes exceed 100 m. Cliffs generally contain a lower geologic unit with more resistant lithified Cenozoic mudstone, shale, sandstone, and siltstone, and an upper unit of weakly lithified Quaternary terrace deposits. Cliffs are usually fronted by a narrow wave-cut platform covered by a thin (and sometimes absent) veneer of sand and cobble. The general coastal setting (cliff, beach, etc.) was characterized using aerial imagery (National Agriculture Imagery Program, 2016), oblique photographs (California Coastal Records Project, 2013), and coastal maps (Griggs et al., 2005). Regional urbanization and infrastructure development have significantly altered the coast and reduced terrestrial sand yield.

Over 40 estuaries, characterized by low volume and intermittent freshwater inflow, line the Southern California study area (Elwany et al., 1998, 2003; Largier, 2010; Largier et al., 1996, 1997). The inlets are exposed to waves that affect their morphodynamics and make them prone to mouth migration and intermittent mouth closure (e.g., Moreno et al., 2010; Zedler, 2010). Unmodified inlets historically migrated seasonally (southward in winter), and in response to individual storms (Engstrom, 2006). However, most Southern California estuary inlets are now stabilized by jetties and bridge abutments, and require maintenance dredging to keep them open at annual costs ranging about $100 K to $1 M per inlet (Elwany et al., 1997; Hastings & Elwany, 2012; Jenkins & Wasyl, 2006; Pratt, 2014). Inlet closures increase occurrences of strong stratification, high phytoplankton biomass, and potentially low oxygen (e.g., Ortega-Cisneros et al., 2014), and create breeding grounds for mosquitoes with a risk of vector-borne diseases.

Waves generated by distant storms undergo a complex transformation before reaching the Southern California coast. Wave shadows of the Channel Islands create strong alongshore variations in wave height on scales of 10 km, and the curvature of the continent shelters the entire coastline to varying degrees from northerly wave approach directions (Pawka, 1983). During the 2015–2016 El Niño, wave direction (mean peak wave direction of top 5% biggest waves) at a Southern California buoy (Oceanside; Figure 1) shifted northerly by 18–24° compared with the 1997–1998 and 2009–2010 El Niños (Barnard et al., 2017). Wave heights in San Diego County during the 2015–2016 El Niño and 2009–2010 El Niños were similar (Ludka et al., 2016), and higher in 1997–1998 (Doria et al., 2016). The mean tide range is 1.1 m, but extreme tropic tides in winter and summer can reach 2.7 m (Zetler & Flick, 1985). Peak winter tides in 2015–2016 occurred early in the season reducing the chance of coinciding with storm waves (Flick, 2016).

The coastal California semiarid Mediterranean climate is characterized by dry summers and occasionally wet winters, with most rainfall between November and March (annual average, 250–300 mm [wrcc.dri.edu]). Precipitation was 30% below average during the study period and significantly less than recent previous El Niños.

## 3. Methods

### 3.1. Lidar

Airborne lidar data sets were collected on 6 October 2015 and 22 March 2016 using the MASS (Modular Aerial Sensing System; Melville et al., 2016; Reineman et al., 2009) outfitted with a Riegl Q680i scanning lidar and Novatel SPAN-LN200 GPS-IMU. Vertical and horizontal lidar point accuracy was estimated from the boresight calibration at 1.8–2.4 and 5.7–11.2 cm, respectively. Lidar data were processed into 1-m resolution digital elevation models. Digital change grids, differences of successive digital elevation models, include errors from the lidar observations, spatial interpolation, and vegetation. The mean and maximum vertical root-mean-square error (RMSZ) of the change grid was estimated at 4 and 15 cm, respectively, using eight control surfaces (assumed stable, average surface area of ~6,000 $m^2$) spread throughout the study area. The vertical RMSZ includes horizontal lidar errors because the control surfaces are sloped (over a representative range).

### 3.2. Waves and Runup

A buoy-driven, regional wave model (O'Reilly et al., 2016) was used to estimate hourly wave conditions in 10-m water depth spaced at 100-m intervals alongshore. The model includes the effects of complex offshore bathymetry and varying beach orientation on wave exposure. Wave data were linearly interpolated to 5-m alongshore resolution.

Total water level (TWL) is the sum of the observed water level at the Los Angeles tide gage (station 9410660) and the vertical height of wave runup (Ruggiero et al., 2001; Shih et al., 1994). Vertical wave runup was approximated as the level exceeded by 2% of wave uprushes (Stockdon et al., 2006, equation (18)). The effect of beach morphology and slope is not included in these estimates. Hourly TWL exceeding 2.5-m elevation (NAVD88) is used here as a measure of erosive conditions.

### 3.3. Beaches

Mean high water (MHW; elevation 1.39 m NAVD88 at Los Angeles) shorelines were extracted from the lidar digital elevation models and used to estimate planimetric and vertical beach changes on cross-shore transects spaced 5 m apart. Vertical beach change was measured at the 22 March 2016 MHW shoreline transect

locations. Beach volume change was evaluated above MHW elevation, between MHW shorelines. MHW was used because mean seal level (MSL) was not exposed sufficiently.

### 3.4. Cliffs

To detect cliff changes, grid cells with a vertical change of less than 30 cm (>RMSZ) were neglected and a minimum 5-$m^2$ footprint was imposed, requiring more than five connected cells of positive or negative change. Changes were then evaluated in 5-m-wide alongshore compartments (see Young, Guza, et al., 2009; Young, Flick, et al., 2009; Young et al., 2010). Dividing the net volumetric compartment change by the cliff height and 5-m compartment width yielded average cliff retreat over the cliff face (Figure S3).

### 3.5. Estuaries

Each estuary inlet was split into three regions: estuary, north beach, and south beach. Beach regions extended 100 m along-coast from the inlet edge. Mean elevation change in beach regions was calculated between the 22 March 2016 MHW line and the back-beach. The studied estuary inlet region extended inland to the coast highway, bridge, or other fixed structure (e.g., Figure 2c). At a few estuaries, the elevation change is underestimated because water covered the beach in the first survey. In total, 45 estuary mouths are identifiable in the lidar data, 28 of which were analyzed (several were too small and/or not covered by both lidar flights) for adjacent beach change. Eleven inlets were covered with water (i.e., fully open) during both surveys, leaving 17 estuaries for full analysis (inlet and north/south beaches).

## 4. Results

### 4.1. Waves and Runup

Southern California mean water levels during the 2015–2016 El Niño (tidesandcurrents.noaa.gov) were consistently superelevated 15–25 cm, with maximum exceedance of up to 39 cm (Figure 3b), similar to previous El Niños (Flick, 2016). On 25 November 2015, the El Niño anomaly, high tides, and the long-term trend in local sea level rise generated record high water levels at San Diego and La Jolla, and the third highest at the Santa Monica and Los Angeles tide stations. Elevated water levels contributed to localized flooding (Figure S1).

Modeled nearshore wave height and total water level varied alongshore with the highest waves on the west and northwest facing locations. Locations facing south were sheltered. Large waves during the study period occurred often during low and moderate tides (Figures 3c and 3d). Incident waves were moderate (2 m at La Jolla) during the highest observed water levels (25 November 2015). High water level (>2 m NAVD88) and large waves coincided only twice (12 December 2015 and 9 January 2016), limiting total peak water elevations (Figure 3e) and erosion. Total water levels varied alongshore similar to modeled wave heights (Figure 4).

### 4.2. Beaches

Average MHW shoreline retreat was 10 m (Figure 4a and Table S1 in the supporting information), with 73% of transects moving landward (Figure 4). Maximum landward and seaward MHW movements were similar (116 and 110 m, respectively). Excluding cliff-backed beaches, the average MHW shoreline retreated 14 m. Further excluding accretion cases, average retreat was 21 m. The mean vertical change at the 22 March 2016 MHW position was −0.9 m. The largest vertical MHW beach elevation decrease, >5 m, was at an artificially built sand berm (Figure 1 (location 3), Figure 2c, and Table S1 in the supporting information).

Cross-shore beach retreat and/or vertical erosion were largest at Imperial Beach, Silver Strand Beach, Ocean Beach, La Jolla Shores (Figure S2), Blacks Beach, and Surfside (Figures 1 (circled locations 2, 3, 5, 6, 7, and 14) and 4g–4i). At Imperial Beach, a 2012 nourishment elongated alongshore and created historically high backshore sand levels in some locations (Ludka et al., 2016), while other areas retreated over 60 m and lowered up to 2.8 m allowing wave overtopping and flooding, similar to previous observations (Gallien, 2016). In northern Ocean Beach (Figure 1, circled location 5), the beach retreated up to 110 m. Maximum beach retreat in La Jolla Shores and Blacks Beach was about 80 m, with maximum elevation decreases of about 2 and 3 m, respectively. Silver Strand Beach and Surfside-Sunset Beach constructed berm erosion volumes (~200–250 $m^3$/m) were an order of magnitude larger than typically observed (~13–18 $m^3$/m; Gallien et al., 2015). In contrast, large seaward beach changes (accretion) occurred immediately north of two harbors (Figure 1, locations 10 and 13), and a creek mouth (Figure 1, location 19).

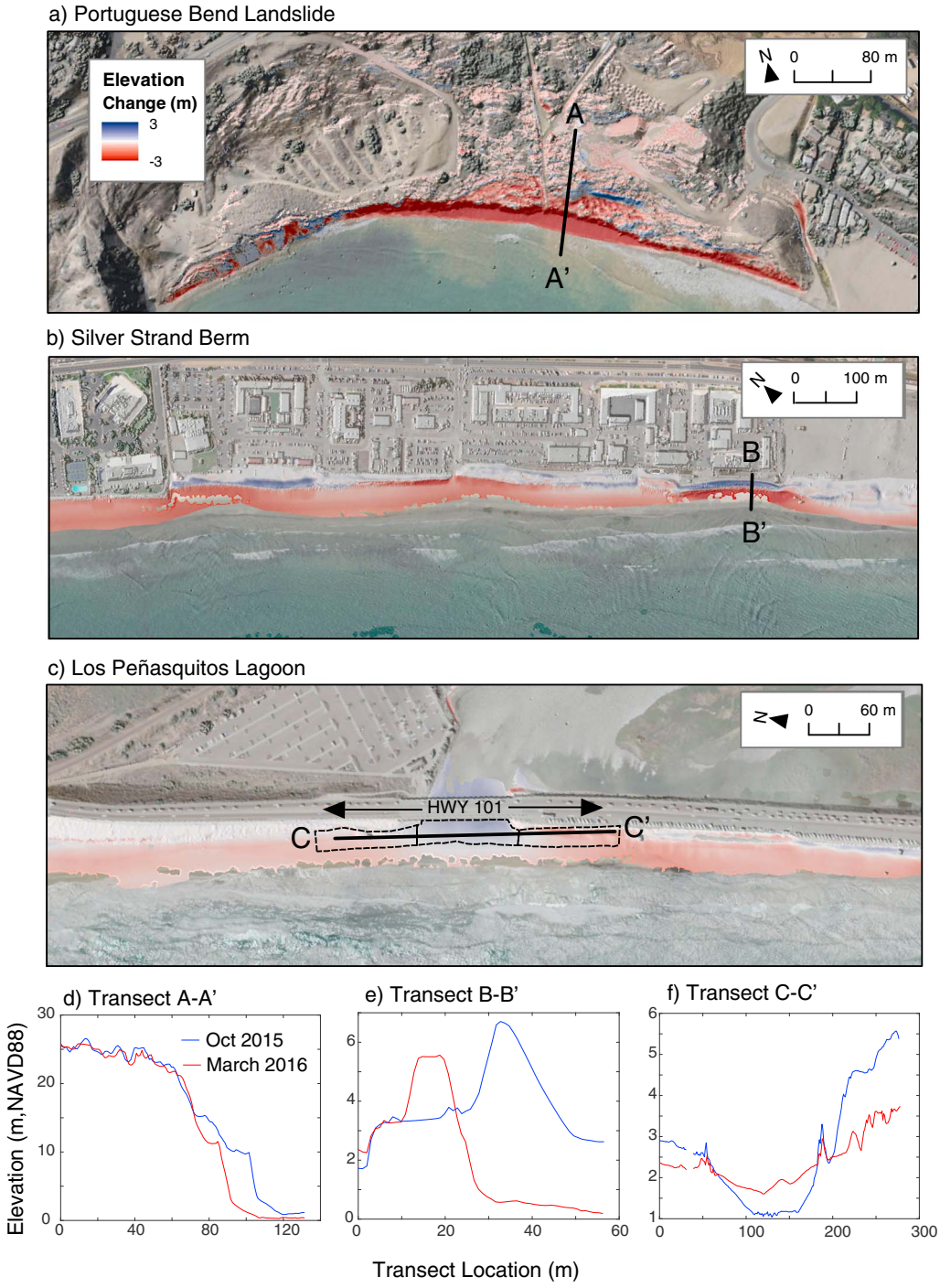


**Figure 2.** Topographic change (6 October 2015 and 22 March 2016; see color bar) at (a) Portuguese bend landslide in Palos Verdes, (b) Silver Strand berm erosion, (c) Los Peñasquitos lagoon inlet accretion/adjacent beach erosion and the Coast Highway 101, and (d–f) corresponding transect elevation. Thin black lines in (c) outline the estuary mouth and adjacent beach regions used in estuary change analysis.

Pocket beaches rotated (Thompson, 1987), notably in Laguna Beach with erosion and accretion at the north (west) and south (east) ends, respectively. Similar erosion patterns often (but not always) occurred around jetties and groins with sand accretion on the north (west) and erosion on the south (east) side. Alternating zones of beach erosion and accretion at scales of about 1,000 m were observed in areas without significant barriers to alongshore sand transport (i.e., groin fields) including Sunset Beach (Figure 4, location 180 km), San

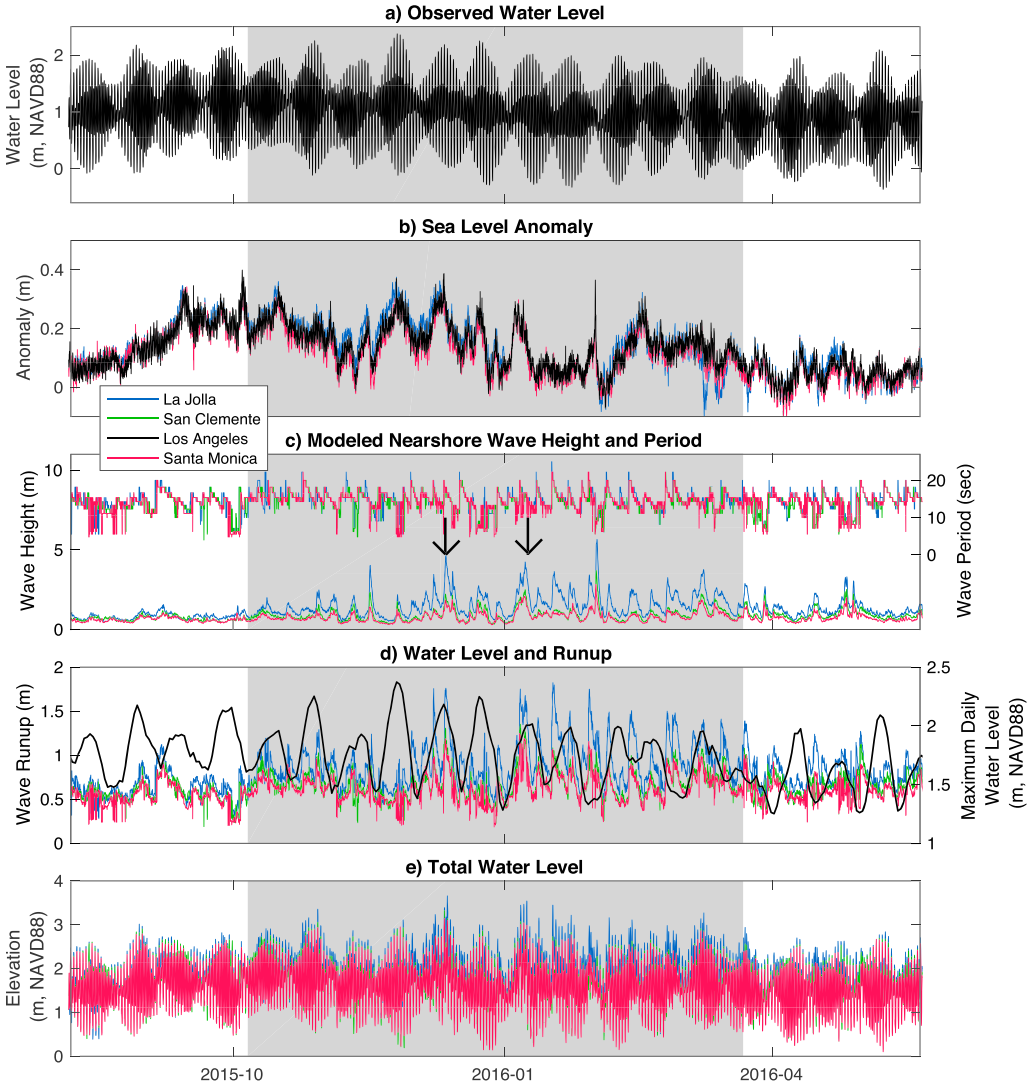


**Figure 3.** Time series of (a) tide gauge water level at Los Angeles, (b) water level anomaly at three locations, (c) modeled nearshore wave height and period, (d) modeled wave runup (and maximum observed daily water level at Los Angeles; dashed black line), and (e) shoreline total water level (TWL) including anomaly and wave superelevation. The study period is gray. Arrows in (d) indicate coincident high tide and high wave events discussed in text. Legend is for all panels.

Clemente (location 128 km), and Camp Pendleton (location 113 km, similar to features previously observed in the area; Reineman et al., 2009). The origin of these features is not understood.

### 4.3. Cliffs

About 12% of cliffs showed topographic change. The average net change was about 1 $m^3/m$ of erosion, equivalent to 3 cm of cliff face retreat. Neglecting armored cliffs, the average net change increases to 1.5 $m^3/m$ of erosion and 4 cm of retreat. The largest observed cliff changes were associated with wave erosion, seaward sliding, and topographic deformation of the Portuguese Bend Landslide (Figure 2a). Cliff erosion occurred primarily at the cliff base. Only two cliff tops retreated significantly: the Portuguese Bend Landslide at Palos Verdes (10–15-m retreat) and a sea-arch failure in Sunset Cliffs (5–10-m retreat). Other substantial backshore erosion or damage included the following: near Los Peñasquitos Lagoon inlet (Figure S1b), San Onofre State Beach, Christmas Tree Cove in Palos Verdes, and Leo Carrillo Parking Lot (Figure 1, circled locations 8, 11, 16, 20). Cliff changes were not spatially correlated with beach changes or total water levels.

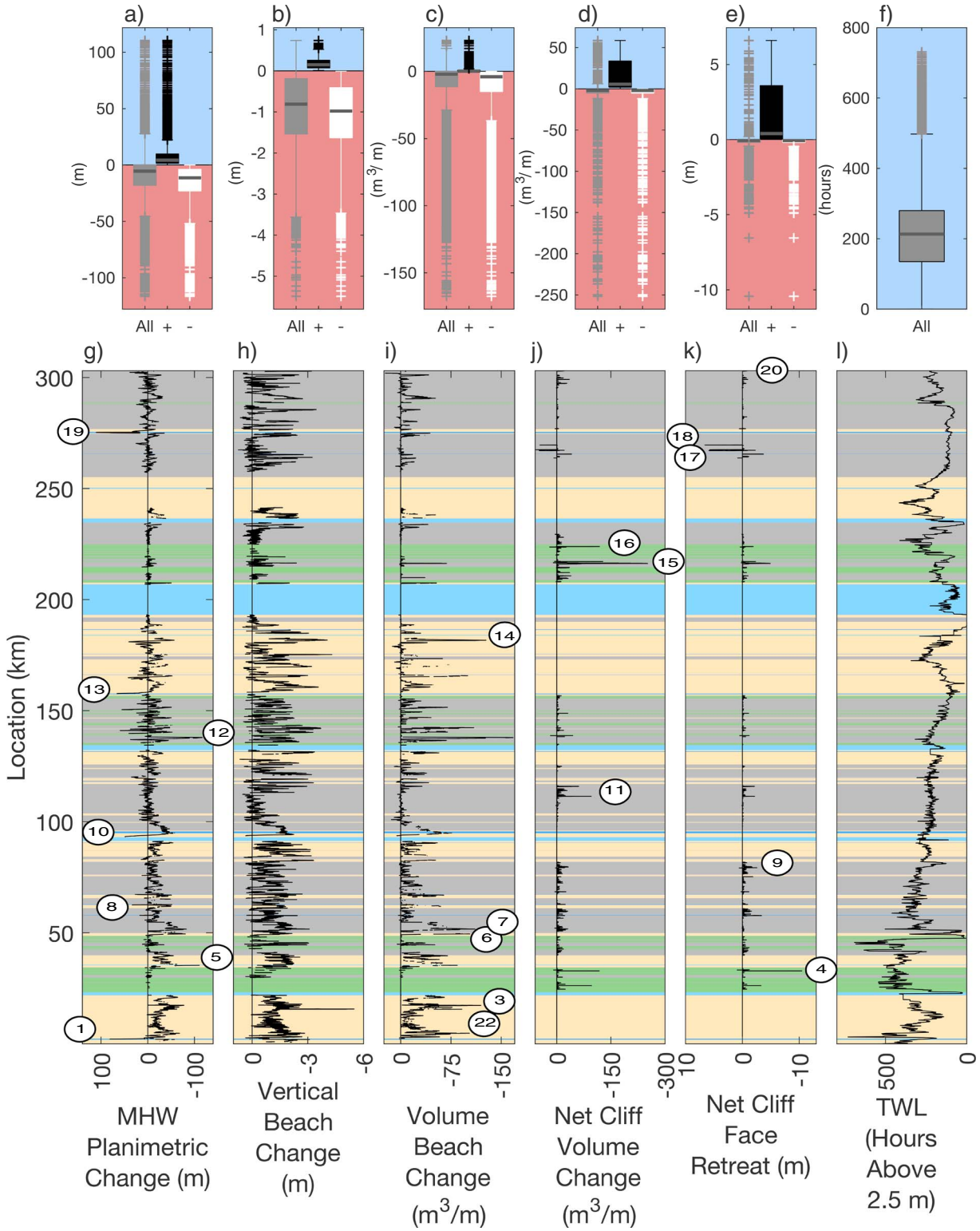


**Figure 4.** Quartile plots (of all values [gray] and separated positive [black] and negative [white] values; upper plots) and alongshore magnitude (lower plots) of (a and g) mean high water (MHW) beach planimetric change; (b and h) vertical beach change at the March MHW location; (c and i) beach volume change above MHW elevation, between MHW shorelines; (d and j) net cliff erosion; (e and k) net cliff face retreat; and (f and l) number of hours with total water level TWL $>$ 2.5 m (NAVD88 datum). Colors (g–l) are beaches (yellow), beaches backed by cliffs (gray), cliffs and rocky coast (green), and harbors and waterways (blue). Location (g–l) is distance from California-Mexico border. Circled numbers are event locations (Figure 1). Quartile plots include the first and third quartiles (filled rectangles), the median, and upper and lower extremes (lines). Outliers (beyond 2.7 standard deviations, i.e., 99%) are indicated with plusses.

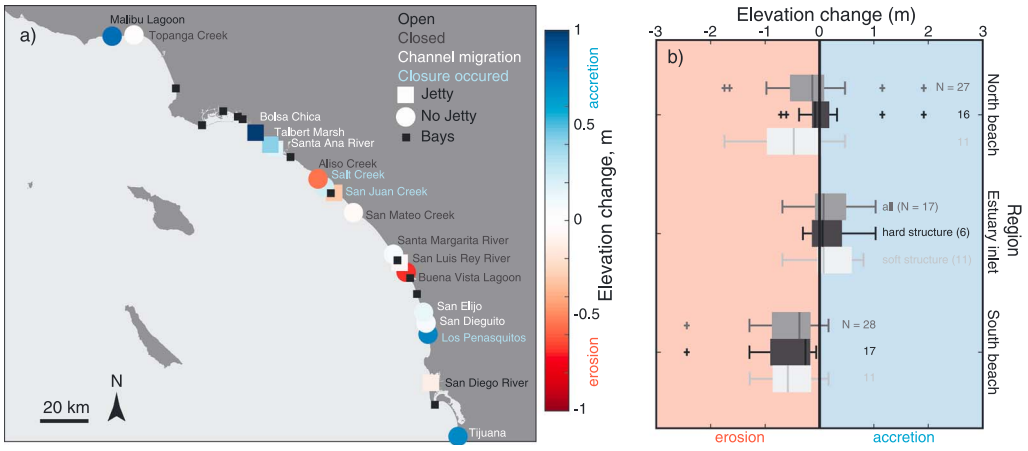


**Figure 5.** (a) Overview of estuary elevation change (6 October 2015 to 22 March 2016): estuary name colors indicate the mouth status during this study (see legend; open in black, closed in gray, channel migration and accretion in white, and mouth closure in blue). Small black squares indicate estuaries for which no estuary region was calculated but adjacent beach regions were calculated (primarily open bays, all of which had jetties or groins at the inlet mouth). Larger colored squares indicate estuaries with structures bordering one or both sides of the inlet. (b) Quartile plots (Figure 4 format) split by estuary regions and presence/absence of structural control.

### 4.4. Estuaries

On average, estuary mouths slightly accreted or remained stable, opposite to erosion on adjacent beaches (Figures 2c and 5). Several inlet areas experienced significant accretion. Of those, three (blue text on Figure 5a) accreted high enough to close between October 2015 and March 2016. A fourth (Tijuana Estuary) closed in April 2016 after the lidar survey. Five estuary mouths were closed throughout the study period, and effectively behaved as beaches (Buena Vista Lagoon, Aliso Creek, San Luis Rey River, San Mateo Creek, and Topanga Creek). Only the San Diego River was both open and eroded. About one third of estuaries analyzed became or remained closed during the sampling period. For those estuaries without groins or jetties (11 total), 64% closed or remained closed. Several estuary mouths with small mean vertical elevation change migrated south (white text; Figure 5a.) Winter closure is not unusual for several of these estuaries; however, it was likely exacerbated by low rainfall (runoff can breach estuary berms; e.g., Behrens et al., 2015; Elwany et al., 1998) and elevated wave and water levels (hypothesized to cause accretion in inlet mouths; e.g., Behrens et al., 2015; Jacobs et al., 2010).

On average, adjacent estuary beaches eroded (Figure 5). At structurally controlled estuaries (e.g., groins, jetties), adjacent beach behavior was generally suggestive of structure interruption of southward alongshore sand transport. On average, the north beach elevation change was near zero, while south beaches were strongly eroded. At lagoons with no stabilizing structures, beaches on both sides usually eroded similarly. Overall, the estuary and adjacent beach analysis resulted in less erosion than the beach MHW methods because the estuary analysis included the wide back-beach that often changed little, or in some cases accreted.

## 5. Historical Perspective

### 5.1. Environmental Variables, Rain, Waves, and Water Levels

During the last 20 years, the highest multivariate ENSO index was in 1997–1998, with 2015–2016 almost as strong (Figure 6a). Rain, waves, and total water level (TWL; including tides, mean sea level enhancements, and waves) all peaked during the 1997–1998 El Niño. Rainfall was below average during 2015–2016, slightly above average in 2009–2010, and extreme in 1997–1998 (Figure 6a). Mean nearshore wave energy and number of hours total water levels exceeded 2.5 m (NAVD88) during the 2015–2016 El Niño were less than the 1997–1998 El Niño event (19% and 25%, respectively), and similar to the 2009–2010 El Niño (Figure 6a). The number of hours total water elevations exceeded 3.5 m were notably lower in all time periods compared to the 1997–1998 El Niño.

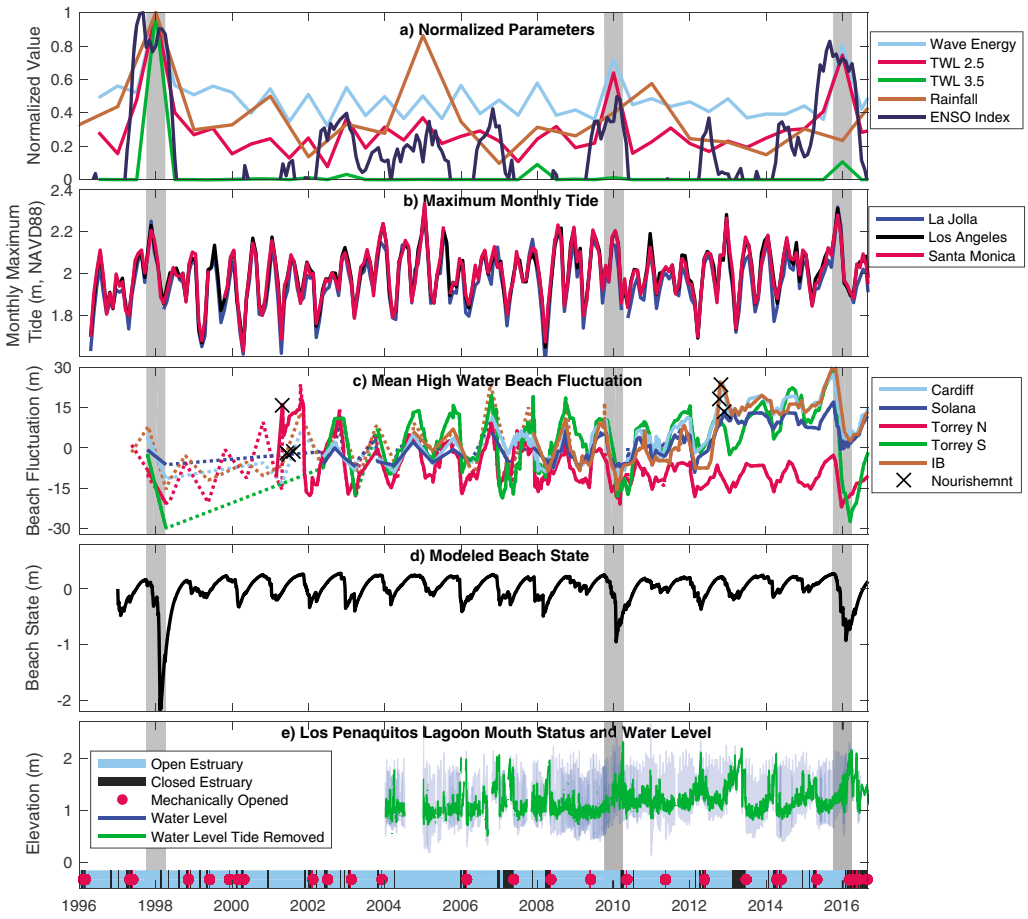


**Figure 6.** Time series of (a) normalized, seasonal mean nearshore wave energy, hour TWL exceeds 2.5 and 3.5 m, Los Angeles water year rainfall, and monthly multivariate El Niño–Southern Oscillation (ENSO) index. (b) La Jolla, Los Angeles, and Santa Monica monthly maximum observed water level excluding wave runup effects. (c) Alongshore averaged beach width (mean high water position) fluctuations for five Southern California beaches (see Figure 1 for locations). (d) Average model beach state for sites shown in (c). (e) Los Peñasquitos lagoon mouth status, mechanical mouth openings, water levels (Tijuana estuary National Estuarine Research Reserve System wide monitoring program), and water levels with tide removed (Godin filtered). In (a), Hs is in 10-m depth, and averaged over seasons (three months) and 300-km alongshore span. Dashed curves in (c) represent spatially sparse surveys from Coastal Frontiers.

Water levels were at or near all-time records during the 2015–2016 El Niño (Figure 6b), yet the total water levels exceeding 3.5 m were about 90% lower than peak values (Figure 6a), suggesting more synchronous timing of high waves and peak tides during the 1997–1998 event. Indeed, high waves often occurred during higher tide conditions in 1997–1998 (Figure 7, top panels), and wave superelevations were much higher than other large recent El Niños. Thus, 1997–1998 El Niño total waters were above both the 2009–2010 and 2015–2016 El Niños.

Offshore waves at the Harvest Buoy (outside the Southern California Bight and Channel Islands; Figure 1) during 2015–2016 El Niño were the highest recorded in the last 20 years. Mean (of the largest 5%) offshore winter wave height and potential runup were all well above average winter levels and similar during the last three major El Niños (Figure 8). Mean wave direction (of the largest 5% waves) were near winter average during the 2009–2010 and 2015–2016 El Niños (296°), but 12° more westerly during the 1997–1998 El Niño (to 284°; Figure 8). The more westerly wave angles of the 1997–1998 El Niño decreased island sheltering and contributed to elevated nearshore wave energies and total water levels (Figure 7).

### 5.2. Beaches

Direct comparison with 2009–2010 El Niño beach change data from Barnard et al. (2017), Ludka et al. (2016), or Doria et al. (2016) is thwarted because of shoreline datum differences (MSL versus MHW). However, over

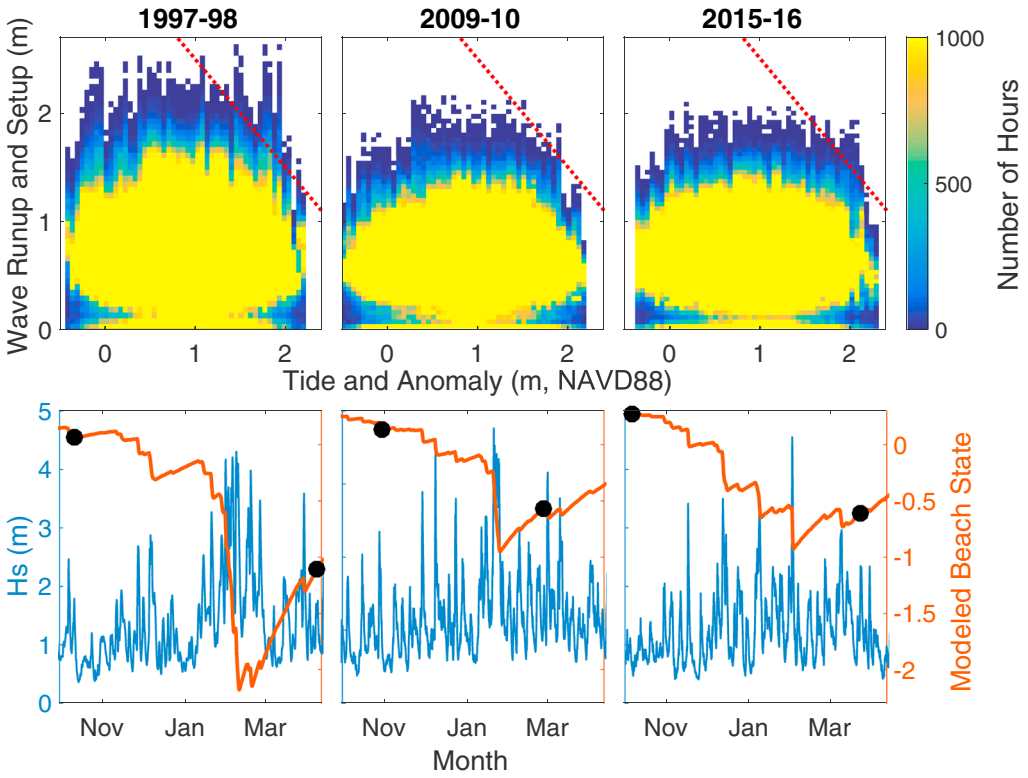


**Figure 7.** (left to right) 1997–1998, 2009–2010, and 2015–2016 El Niños. (top) Number of hours (see color bar) for co-occurring wave superelevation (runup and setup; Stockdon et al., 2006) and tidal (including regional anomalies) level. Hourly waves are in 10-m depth, at 100-m intervals over the 300-km study span. Dashed red line is total water level TWL = 3.5 m, the sum of the water level (excluding waves), and the wave superelevation (runup and setup). (bottom) Significant wave height Hs (blue, in 10-m depth, averaged over San Diego beaches shown in Figure 6c), and modeled beach state (red) from Figure 6d. Black dots show lidar survey dates. Substantial beach recovery may have occurred before the March 1998 survey.

the common reach (Long Beach to the international border, 195 km), the 2015–2016 El Niño MHW and previous 2009–2010 MSL (Doria, 2016) changes were similar with mean shoreline change and percentage of accreted transects −12.7 to −12.9 m and 22–23%, respectively. Four of five San Diego beaches were narrower (2–18 m) during 1997–1998 than 2015–2016 (Figure 6c).

In the crenulated reach between locations 100–200 km (Figure 4), 36% of the shoreline accreted with mean retreat of only −5 m. This differs from Barnard et al. (2017) because the continuous shoreline was analyzed at high resolution compared to their few select sites (total 300 versus 14 km). Furthermore, four of the five Southern California beaches in Barnard et al. (2017) (same sites as in Figure 6c and locations in Figure 1) were recently nourished, and are not necessarily representative of the broader coastline. Southern California beach erosion during the 2015–2016 El Niño was more varied than suggested previously.

An empirical beach state model (Ludka et al., 2015; Yates, Guza, & O'Reilly, 2009; Figure 6d) previously calibrated at sites shown in Figure 6c as well as at Camp Pendleton, estimates erosion potential of the observed waves using equilibrium concepts (Wright et al., 1985; Wright & Short, 1984). Hourly waves alongshore averaged over each monitoring site in Figure 6c, then averaged across all sites are used as model input. The beach state A characterizes the seasonal sand exchange between summer berm ($A > 0$) and winter bar ($A < 0$). The rate of change of the beach state

$$\frac{dA}{dt} = C^{\pm}E^{1/2}\Delta E$$

depends on both the incident wave energy, $E$, and wave energy disequilibrium,

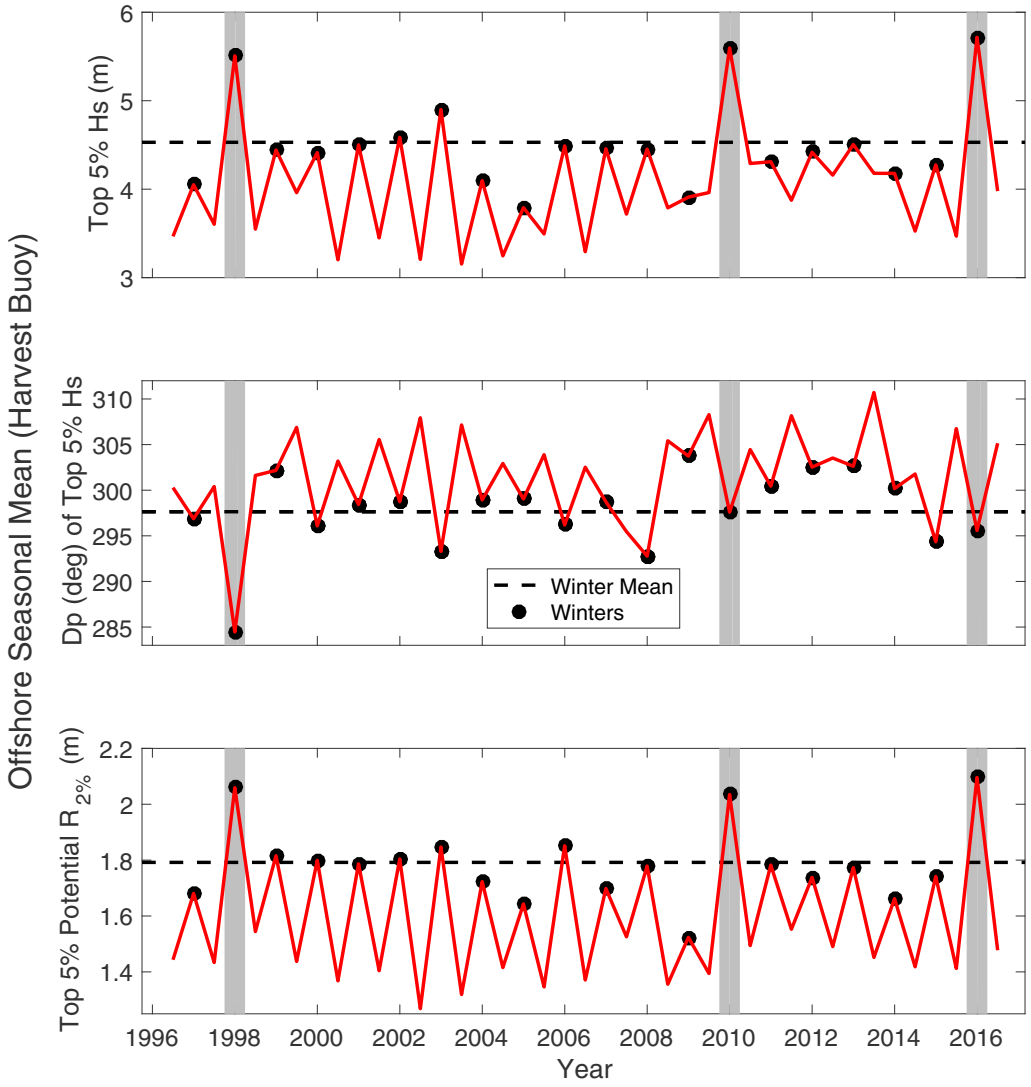


**Figure 8.** Offshore Harvest buoy seasonal time series of (top) mean significant wave height of largest 5% waves, (middle) mean peak direction of largest 5% waves, and (bottom) mean potential wave runup of highest 5%. Black dots are winter seasons and dashed black line is the winter seasonal mean.

$$\Delta E = E - E_{eq}$$

where

$$E_{eq} = aA + b$$

The equilibrium energy $E_{eq}$ is the wave energy that causes no profile change for a given beach state. A single set of optimized parameters for change rate coefficients $C^+$ and $C^-$ (used for beach face accretion and erosion, respectively), and equilibrium energy slope and intercept $a$ and $b$, were found for times and locations not detectibly influenced by nourishment, reef, canyon, shoal, or lagoon mouth, within the intensive monitoring effort (Ludka et al., 2015). The model reasonably reproduced profile observations during unnourished times at all selected sites, shown to behave similarly; however, these curated sections of beach cumulatively span less than 10 km, and are all in the southernmost third of the 300-km domain investigated in the present study. Grain size varies within the Southern California bight (Yates, Guza, O'Reilly, & Seymour, 2009) and influences model parameters (Yates et al., 2011); therefore, this beach state estimate may not be representative of

the broader coastline. The model also does not account for increased erosion resistance of underlying bedrock or cobbles during extreme events, often overpredicting erosion during El Niño winters (Doria et al., 2016). Despite these caveats, an equilibrium model serves as one of the best available wave-driven estimates of multiyear sandy beach evolution, reproducing both erosion of successive storms and recovery between storms. At these sites, during the 20-year study period, the equilibrium model predicts that the waves of the 1997–1998 El Niño winter had the largest wave potential to cut back beach widths, followed by Niño winters in 2009–2010 and 2015–2016 winters (Figures 6d and 7, bottom panel). Furthermore, the model quantifies the suggestion (Barnard et al., 2017) that 1998 lidar flight missed the peak erosion while the 2010 and 2016 flights were better timed (Figure 7, bottom panels).

### 5.3. Cliffs

Despite depleted winter beaches in many areas, cliff erosion was limited probably because the few large wave events did not occur during the highest tides (Figure 3) and because of below average precipitation, consistent with previous studies (Young, 2015; Young, Guza, et al., 2009). The average cliff face and cliff top retreat was 3 cm, and near zero, respectively, less than long-term historical cliff top rates of 5–25 cm/year (Hapke et al., 2009; Young, 2018) and low compared to mean short-term retreat rates of 1–15 cm/year (Young, 2018; Young et al., 2011; Young & Ashford, 2006; Young, Flick, et al., 2009). Limited cliff erosion could also be attributed to the relatively small volumes associated with basal erosion compared to larger upper cliff failures (the latter often triggered by rainfall).

### 5.4. Estuaries

In Los Peñasquitos Lagoon, approximate closure and dredging dates go back to 1965 (Hastings & Elwany, 2012) and show increased closures during the 2015–2016 El Niño relative to the last 20 years (Figure 6e). The Tijuana Estuary closed for the first time during the 2015–2016 El Niño since the major El Niño of 1982–1983. However, quantitative historical context for the inlet accretion across the region during the 2015–2016 El Niño is lacking because Southern California estuaries are subject to slightly different wave action and river flows (Jacobs et al., 2010), are heavily managed (Pratt, 2014), and historical records are deficient. Dredged amounts and accurate locations of dredging and fill operations are often unknown. Nevertheless, as it is expected that elevated wave and water levels cause accretion in inlet mouths (e.g., Behrens et al., 2015; Jacobs et al., 2010) while large river outflows can breach estuary berms (e.g., Behrens et al., 2015; Elwany et al., 1998), the high wave, yet low precipitation during the 2015–2016 El Niño would be conducive to estuary inlet accretion as was observed.

## 6. ENSO Discussion

El Niño and other climate cycles influence coastal conditions around the Pacific. Barnard et al. (2015) found the contrasting coastal behavior observed on opposite sides of the Pacific most closely follows ENSO compared to other climate indices. However, El Niño characteristics can vary considerably (Capotondi et al., 2015) and associated wave energy levels and storm surges differ widely (Bromirski et al., 2005, 2017). Kao and Yu (2009) broadly categorize El Niño events by the location of the major sea surface warming anomaly: Eastern Pacific (canonical; e.g., 1997–1998) and central Pacific (e.g., 2009–2010). Previous strong El Niño events (e.g., 1982–1983, 1997–1998) were Eastern Pacific focused; however, the 2015–2016 El Niño was a mixed Eastern and central Pacific event, which L'Heureux et al. (2017) described as "approximately in the middle of the ENSO continuum."

A comparison of the last three strong El Niño events (1982–1983, 1997–1998, 2015–2016) by Siler et al. (2017) found that while all three events had classically elevated water temperatures in the Eastern Pacific, the 2015–2016 event had other tropical sea surface anomalies unrelated to El Niño. The atmospheric response to these anomalies pushed the storm track farther north limiting rainfall in Southern California. Jong et al. (2018) also compared the last three strong El Niño events (1982–1983, 1997–1998, 2015–2016) and found that during the 2015–2016 event the maximum SST anomaly was further west compared to 1982–1983 and 1997–1998. This possibly prevented the classical teleconnections that deliver elevated rainfall to California. Bromirski et al. (2017) suggest that changes in the Hadley circulation possibly limited storm surge during the 2015–2016 event compared to other El Niño events. These characteristics make the 2015–2016 El Niño event unusual compared with earlier recorded strong canonical El Niño events where storm tracks are

shifted south, creating a more westerly wave approach, generally greater wave exposure, and increased rainfall for Southern California.

Adams et al. (2008) found that Southern California deepwater waves during previous El Niños coinciding with a warm phase PDO are larger, have longer periods, and are shifted more westerly compared to a cool phase PDO. In portions of Southern California, these wave differences can cause significant changes in nearshore wave heights (Adams et al., 2008), longshore sediment transport patterns, and erosional hot spot locations (Adams et al., 2011). The 2015–2016 El Niño coincided with a positive warm phase PDO index (http://research.jisao.washington.edu/pdo/). The large waves observed during 2015–2016 El Niño were consistent with previous warm PDO phase El Niños; however, the westerly shift in wave direction was not observed, highlighting the unusual behavior of the 2015–2016 El Niño.

Climate and ocean modeling considering future climate change suggest a poleward shift of storm tracks and winds in the northern Pacific Ocean, and a decrease in wave energy in Southern California (Cayan et al., 2009; Erikson et al., 2015; Graham et al., 2013). However, this should not detract from the expected increase in flood events in Southern California from rising sea levels (Tebaldi et al., 2012). The modeled future wave changes associated with more northerly winter storm activity are more similar to the 2015–2016 El Niño event compared to canonical El Niño events when wave approach is more westerly. Collins et al. (2010) and Stevenson (2012) highlight the statistical difficulty in estimating changes in future ENSO patterns due to climate change; however, Cai et al. (2014) estimate an increase in frequency of strong El Niño events. Therefore, the 2015–2016 El Niño, both a strong event and one associated with more northerly wave generation, may provide some insight into future oceanographic forcing conditions and coastal storm response in Southern California.

The observed northerly wave approach during the 2015–2016 El Niño and the associated coastal response in Southern California is consistent with research (Harley et al., 2017; Mortlock et al., 2017) in other regions highlighting the importance of incident storm wave direction on beach response, where regions typically sheltered to storm waves become exposed and vice versa. The expected poleward shift of storm tracks under climate change suggest that shorelines sensitive to incident wave direction could experience modified equilibrium beach states, longshore transport, and seasonal erosion patterns, particularly in regions with a variety of shoreline orientations such as local embayments and bights.

## 7. Summary

The 2015–2016 El Niño, one of the strongest on record as measured by the multivariate ENSO index, caused widespread damage and erosion on the U.S. West Coast. The observed 15–25-cm superelevation of water levels (not including wave effects) were equivalent to several decades of projected sea level rise. However, the 2015–2016 El Niño was not a canonical El Niño event and Southern California was often sheltered from notably energetic offshore waves by the northerly wave approach direction, and the large swell that did occur was not synchronous with the highest tides. Airborne lidar surveys spanning 300 km of Southern California coast show the response varied from considerable erosion, to no change, to accretion. On average, the shoreline moved landward 10 m, similar to the 2009–2010 El Niño. Beach retreat exceeded 80 m at a few locations. However, 27% of the shoreline accreted, often in pocket beaches, or near jetties. Over a 100-km reach of crenulated shoreline, 36% of the shoreline accreted. About one third of estuaries analyzed remained closed or became closed. On average, estuaries accreted while their adjacent beaches eroded. Only 12% of cliffs eroded (mostly at the base) and average cliff face retreat was markedly less than historical values. Only two cliff-top areas retreated significantly, and backshore infrastructure damage was minimal. Below average rainfall probably contributed to increased estuary closures and limited cliff erosion.

## Author Contributions

A.P.Y. prepared the original manuscript. A.P.Y., T.W.G., M.H., B.C.L., S.N.G., and W.C.O. conducted the data analysis. L.L. and W.K.M. collected the lidar data. All authors contributed to data interpretation and manuscript editing.

**Acknowledgments**

We thank Nick Statom for his tireless efforts in operating the MASS system, and the pilots and crew at Aspen Helicopters for their skilled flying and aircraft operations. A.P.Y. was funded by the California Department of Parks and Recreation, Division of Boating and Waterways (DPR-DBW), and the United States Army Corps of Engineers (USACE). L.L., W.K.M., and lidar flights were funded by ONR grant (N00014-15-1-2871) to W.K.M. Lidar data analysis and wave data (as part of the Coastal Data Information Program) were funded by DPR-DBW and USACE. The lidar data used in this publication are available at the UCSD Library Digital Collections (https://library.ucsd.edu/dc). Other data used are listed in the references, tables, and supporting information. Estuary analysis was partially funded by the University of Southern California Sea Grant 75193327 and the California Department of Parks and Recreation Division of Boating and Waterways Oceanography Program under contract C1670005 with Scripps Institution of Oceanography.

## References

Adams, P. N., Inman, D. L., & Graham, N. E. (2008). Southern California deep-water wave climate: Characterization and application to coastal processes. *Journal of Coastal Research*, *244*, 1022–1035. https://doi.org/10.2112/07-0831.1

Adams, P. N., Inman, D. L., & Lovering, J. L. (2011). Effects of climate change and wave direction on longshore sediment transport patterns in Southern California. *Climatic Change*, *109*(S1), 211–228. https://doi.org/10.1007/s10584-011-0317-0

Barnard, P. L., Allan, J., Hansen, J. E., Kaminsky, G. M., Ruggiero, P., & Doria, A. (2011). The impact of the 2009–10 El Niño Modoki on US West Coast beaches. *Geophysical Research Letters*, *38*, L13604. https://doi.org/10.1029/2011GL047707

Barnard, P. L., Hoover, D., Hubbard, D. M., Snyder, A., Ludka, B. C., Allan, J., et al. (2017). Extreme oceanographic forcing and coastal response due to the 2015–2016 El Niño. *Nature Communications*, *8*, 14,365. https://doi.org/10.1038/ncomms14365

Barnard, P. L., Short, A. D., Harley, M. D., Splinter, K. D., Vitousek, S., Turner, I. L., et al. (2015). Coastal vulnerability across the Pacific dominated by El Niño/Southern Oscillation. *Nature Geoscience*, *8*(10), 801–807. https://doi.org/10.1038/ngeo2539

Behrens, D. K., Brennan, M., & Battalio, B. (2015). A quantified conceptual model of inlet morphology and associated lagoon hydrology. *Shore & Beach*, *83*, 1–10.

Bromirski, P. D., Cayan, D. R., & Flick, R. E. (2005). Wave spectral energy variability in the Northeast Pacific. *Journal of Geophysical Research*, *110*, C03005. https://doi.org/10.1029/2004JC002398

Bromirski, P. D., Flick, R. E., & Cayan, D. R. (2003). Storminess variability along the California coast: 1858–2000. *Journal of Climate*, *16*(6), 982–993. https://doi.org/10.1175/1520-0442(2003)016<0982:SVATCC>2.0.CO;2

Bromirski, P. D., Flick, R. E., & Miller, A. J. (2017). Storm surge along the Pacific coast of North America. *Journal of Geophysical Research: Oceans*, *122*, 441–457. https://doi.org/10.1002/2016JC012178

Cai, W., Borlace, S., Lengaigne, M., Van Rensch, P., Collins, M., Vecchi, G., et al. (2014). Increasing frequency of extreme El Niño events due to greenhouse warming. *Nature Climate Change*, *4*(2), 111–116. https://doi.org/10.1038/nclimate2100

California Coastal Records Project (2013). Kenneth and Gabrielle Adelman, www.Californiacoastline.org

Capotondi, A., Wittenberg, A. T., Newman, M., Di Lorenzo, E., Yu, J. Y., Braconnot, P., et al. (2015). Understanding ENSO diversity. *Bulletin of the American Meteorological Society*, *96*(6), 921–938. https://doi.org/10.1175/BAMS-D-13-00117.1

Cayan, D., Bromirski, P., Hayhoe, K., Tyree, M., Dettinger, M., & Flick, R. (2008). Climate change projections of sea level extremes along the California coast. *Climatic Change*, *87*(S1), 57–73. https://doi.org/10.1007/s10584-007-9376-7

Cayan, D. R., Tyree, M., Dettinger, M. D., León, H., Hugo, G., Das, T., et al. (2009). Climate change scenarios and sea level rise estimates for California 2008 Climate Change Scenarios Assessment.

Collins, M., An, S. I., Cai, W., Ganachaud, A., Guilyardi, E., Jin, F. F., et al. (2010). The impact of global warming on the tropical Pacific Ocean and El Niño. *Nature Geoscience*, *3*(6), 391–397. https://doi.org/10.1038/ngeo868

Doria, A. (2016). Observations and modeling of Southern California beach sand level changes, Ph.D. Dissertation, University of California San Diego, U.S.A.

Doria, A., Guza, R. T., O'Reilly, W. C., & Yates, M. L. (2016). Observations and modeling of San Diego beaches during El Niño. *Continental Shelf Research*, *124*, 153–164. https://doi.org/10.1016/j.csr.2016.05.008

Elwany, M. H. S., Flick, R. E., & Aijaz, S. (1998). Opening and closure of a marginal Southern California lagoon inlet. *Estuaries*, *21*(2), 243–251.

Elwany, M. H. S., Flick, R. E., & Hamilton, M. (2003). Effect of a small Southern California lagoon entrance on adjacent beaches. *Estuaries*, *26*(3), 700–708. https://doi.org/10.1007/BF02711981

Elwany, M. H. S., Thum, A. B., Aijaz, S., Boland, J. M., & Flick, R. E. (1997). A strategy to maintain tidal flushing in small coastal lagoons, Proc. California and the World Ocean, 1265–1277.

Engstrom, W. N. (2006). Nineteenth century coastal geomorphology of Southern California. *Journal of Coastal Research*, *22*(4), 847–861.

Erikson, L. H., Hegermiller, C. A., Barnard, P. L., Ruggiero, P., & van Ormondt, M. (2015). Projected wave conditions in the eastern North Pacific under the influence of two CMIP5 climate scenarios. *Ocean Modelling*, *96*, 171–185. https://doi.org/10.1016/j.ocemod.2015.07.004

Flick, R. E. (1998). Comparison of California tides, storm surges, and mean sea level during the El Niño winters of 1982–83 and 1997–98. *Shore & Beach*, *66*(3), 7–11.

Flick, R. E. (2016). California tides, sea level, and waves—Winter 2015–16. *Shore & Beach*, *84*(2), 25–30.

Gallien, T. W. (2016). Validated coastal flood modeling at Imperial Beach, California: Comparing total water level, empirical and numerical overtopping methodologies. *Coastal Engineering*, *111*, 95–104.

Gallien, T. W., O'Reilly, W. C., Flick, R. E., & Guza, R. T. (2015). Geometric properties of anthropogenic flood control berms on Southern California beaches. *Ocean and Coastal Management*, *105*, 37–45.

Graham, N. E., Cayan, D. R., Bromirski, P. D., & Flick, R. E. (2013). Multi-model projections of twenty-first century North Pacific winter wave climate under the IPCC A2 scenario. *Climate Dynamics*, *40*(5–6), 1335–1360. https://doi.org/10.1007/s00382-012-1435-8

Griggs, G. B., Patsch, K., & Savoy, L. E. (2005). *Living With the Changing California Coast*. Berkeley: University of California Press.

Hapke, C. J., Reid, D., & Richmond, B. (2009). Rates and trends of coastal change in California and the regional behavior of the beach and cliff system. *Journal of Coastal Research*, *25*(3), 603–615.

Harley, M. D., Turner, I. L., Kinsela, M. A., Middleton, J. H., Mumford, P. J., Splinter, K. D., et al. (2017). Extreme coastal erosion enhanced by anomalous extratropical storm wave direction. *Scientific Reports*, *7*(1), 6033. https://doi.org/10.1038/s41598-017-05792-1

Hastings, M., & Elwany, M. H. S. (2012). Managing the inlet at Los Peñasquitos Lagoon. *Shore & Beach*, *80*(1), 9–18.

Huang, B., L'Heureux, M., Hu, Z.-Z., & Zhang, H.-M. (2016). Ranking the strongest ENSO events while incorporating SST uncertainty. *Geophysical Research Letters*, *43*, 9165–9172. https://doi.org/10.1002/2016GL070888

Jacobs, D., Stein, E. D., & Longcore, T. (2010). Classification of California estuaries based on natural closure patterns: Templates for restoration and management. *Southern California Coastal Water Research Project*, *619*, 1–50.

Jenkins, S. A. & Wasyl, J. (2006). Coastal processes effects of reduced intake flows at Agua Hedionda Lagoon, report.

Jong, B. T., Ting, M., Seager, R., Henderson, N., & Lee, D. E. (2018). Role of equatorial Pacific SST forecast error in the late winter California precipitation forecast for the 2015/16 El Niño. *Journal of Climate*, *31*(2), 839–852. https://doi.org/10.1175/JCLI-D-17-0145.1

Kao, H. Y., & Yu, J. Y. (2009). Contrasting eastern-Pacific and central-Pacific types of ENSO. *Journal of Climate*, *22*(3), 615–632. https://doi.org/10.1175/2008JCLI2309.1

Largier, J. L. (2010). Low-inflow estuaries: Hypersaline, inverse, and thermal scenarios. In A. Valle-Levinson (Ed.), *Contemporary Issues in Estuarine Physics* (pp. 247–272). Cambridge: Cambridge University Press.

Largier, J. L., Hearn C. J., and Chadwick D. B. (1996), Density structures in "low-inflow estuaries," in *Buoyancy Effects on Coastal and Estuarine Dynamics* edited by D. G. Aubrey and C. T. Friedrichs, 227-241, Chichester: Wiley.

Largier, J. L., Smith, S. V., & Hollibaugh, J. T. (1997). Seasonally hypersaline estuaries in Mediterranean-climate regions. *Estuarine, Coastal and Shelf Science*, *45*(6), 789–797. https://doi.org/10.1006/ecss.1997.0279

L'Heureux, M. L., Takahashi, K., Watkins, A. B., Barnston, A. G., Becker, E. J., Di Liberto, T. E., et al. (2017). Observing and predicting the 2015/16 El Niño. *Bulletin of the American Meteorological Society*, *98*(7), 1363–1382. https://doi.org/10.1175/BAMS-D-16-0009.1

Ludka, B. C., Gallien, T. W., Crosby, S. C., & Guza, R. T. (2016). Mid-El Niño erosion at nourished and unnourished Southern California beaches. *Geophysical Research Letters*, *43*, 4510–4516. https://doi.org/10.1002/2016GL068612

Ludka, B. C., Guza, R. T., O'Reilly, W. C., & Yates, M. L. (2015). Field evidence of beach profile evolution toward equilibrium. *Journal of Geophysical Research: Oceans*, *120*, 7574–7597. https://doi.org/10.1002/2015JC010893

Melville, W. K., Lenain, L., Cayan, D. R., Kahru, M., Kleissl, J. P., Linden, P., & Statom, N. M. (2016). The modular aerial sensing system. *Journal of Atmospheric and Oceanic Technology*, *33*(6), 1169–1184. https://doi.org/10.1175/JTECH-D-15-0067.1

Moreno, I. M., Ávila, A., & Losada, M. Á. (2010). Morphodynamics of intermittent coastal lagoons in southern Spain: Zahara de los Atunes. *Geomorphology*, *121*(3–4), 305–316. https://doi.org/10.1016/j.geomorph.2010.04.028

Mortlock, T. R., Goodwin, I. D., McAneney, J. K., & Roche, K. (2017). The June 2016 Australian East Coast low: Importance of wave direction for coastal erosion assessment. *Water*, *9*(2), 121.

National Agriculture Imagery Program (2016). USDA's Farm Service Agency, Aerial Photography Field Office, Salt Lake City, Utah, USA.

O'Reilly, W. C., Olfe, C., Seymour, R. J., Thomas, J., & Guza, R. T. (2016). The California coastal wave monitoring and prediction system. *Coastal Engineering*, *116*, 118–132. https://doi.org/10.1016/j.coastaleng.2016.06.005

Ortega-Cisneros, K., Scharler, U. M., & Whitfield, A. K. (2014). Inlet mouth phase influences density, variability and standing stocks of plankton assemblages in temporarily open/closed estuaries. *Estuarine, Coastal and Shelf Science*, *136*(0), 139–148. https://doi.org/10.1016/j.ecss.2013.11.021

Pawka, S. S. (1983). Island shadows in wave directional spectra. *Journal of Geophysical Research*, *88*(C4), 2579–2591. https://doi.org/10.1029/JC088iC04p02579

Pratt, J. (2014). California inlets: A coastal management "No Man's Land," report for the Surfrider Foundation, http://public.surfrider.org/files/CA_Inlet_Report_2014.pdf

Reineman, B. D., Lenain, L., Castel, D., & Melville, W. K. (2009). A portable airborne scanning lidar system for ocean and coastal applications. *Journal of Atmospheric and Oceanic Technology*, *26*(12), 2626–2641.

Ruggiero, P., Komar, P. D., McDougal, W. G., Marra, J. J., & Beach, R. A. (2001). Wave runup, extreme water levels and the erosion of properties backing beaches. *Journal of Coastal Research*, *17*, 407–419.

Sallenger, A. H., Krabill, W., Brock, J., Swift, R., Manizade, S., & Stockdon, H. (2002). Sea-cliff erosion as a function of beach changes and extreme wave runup during the 1997–1998 El Niño. *Marine Geology*, *187*(3-4), 279–297. https://doi.org/10.1016/S0025-3227(02)00316-X

Shih, S. M., Komar, P. D., Tillotson, K. J., McDougal, W. G., & Ruggiero, P. (1994). Wave run-up and sea-cliff erosion, Coastal Engineering 1994 Proceedings, 24th International Conference, American Society of Civil Engineers, *2170–2184*.

Siler, N., Kosaka, Y., Xie, S. P., & Li, X. (2017). Tropical ocean contributions to California's surprisingly dry El Niño of 2015/16. *Journal of Climate*, *30*(24), 10067–10079. https://doi.org/10.1175/JCLI-D-17-0177.1

Stevenson, S. L. (2012). Significant changes to ENSO strength and impacts in the twenty-first century: Results from CMIP5. *Geophysical Research Letters*, *39*, L17703. https://doi.org/10.1029/2012GL052759

Stockdon, H. F., Holman, R. A., Howd, P. A., & Sallenger, A. H. Jr. (2006). Empirical parameterization of setup, swash, and runup. *Coastal Engineering*, *53*(7), 573–588. https://doi.org/10.1016/j.coastaleng.2005.12.005

Storlazzi, C. D., & Griggs, G. B. (2000). Influence of El Niño–Southern Oscillation (ENSO) events on the evolution of Central California's shoreline. *Geological Society of America Bulletin*, *112*(2), 236–249. https://doi.org/10.1130/0016-7606(2000)112<236:IOENOE>2.0.CO;2

Strolazzi, C., Willis, C., & Griggs, G. (2000). Comparative impacts of the 1982–83 and 1997–98 El Niño winters on central California. *Journal of Coastal Research*, *16*, 1022–1036.

Tebaldi, C., Strauss, B. H., & Zervas, C. E. (2012). Modelling sea level rise impacts on storm surges along US coasts. *Environmental Research Letters*, *7*(1), 014032. https://doi.org/10.1088/1748-9326/7/1/014032

Thompson, W. C. (1987). Seasonal orientation of California beaches. *Shore & Beach*, *55*(3–4), 67–70.

Wolter, K., & Timlin, M. S. (2011). El Niño/Southern Oscillation behaviour since 1871 as diagnosed in an extended multivariate ENSO index (MEI.Ext). *International Journal of Climatology*, *31*(7), 1074–1087. https://doi.org/10.1002/joc.2336

Wright, L. D., & Short, A. D. (1984). Morphodynamic variability of surf zones and beaches: A synthesis. *Marine Geology*, *56*(1-4), 93–118. https://doi.org/10.1016/0025-3227(84)90008-2

Wright, L. D., Short, A. D., & Green, M. O. (1985). Short-term changes in the morphodynamic states of beaches and surf zones: An empirical predictive model. *Marine Geololgy*, *62*(3-4), 339–364. https://doi.org/10.1016/0025-3227(85)90123-9

Yates, M. L., Guza, R. T., & O'Reilly, W. C. (2009). Equilibrium shoreline response: Observations and modeling. *Journal of Geophysical Research*, *114*, C09914. https://doi.org/10.1029/2009JC005359

Yates, M. L., Guza, R. T., O'Reilly, W. C., Hansen, J. E., & Barnard, P. L. (2011). Equilibrium shoreline response of a high wave energy beach. *Journal of Geophysical Research*, *116*, C04014. https://doi.org/10.1029/2010JC006681

Yates, M. L., Guza, R. T., O'Reilly, W. C., & Seymour, R. J. (2009). Overview of seasonal sand level changes on Southern California beaches. *Shore & Beach*, *77*, 39–46.

Young, A. P. (2015). Recent deep-seated coastal landsliding at San Onofre State Beach, California. *Geomorphology*, *228*, 200–212. https://doi.org/10.1016/j.geomorph.2014.08.005

Young, A. P. (2018). Decadal-scale coastal cliff retreat in Southern and central California. *Geomorphology*, *300*, 164–175. https://doi.org/10.1016/j.geomorph.2017.10.010

Young, A. P., & Ashford, S. A. (2006). Application of airborne lidar for seacliff volumetric change and beach-sediment budget contributions. *Journal of Coastal Research*, *222*, 307–318. https://doi.org/10.2112/05-0548.1

Young, A. P., Flick, R. E., Gutierrez, R., & Guza, R. T. (2009). Comparison of short-term seacliff retreat measurement methods in Del mar, California. *Geomorphology*, *112*(3–4), 318–323. https://doi.org/10.1016/j.geomorph.2009.06.018

Young, A. P., Guza, R. T., C, W., O'Reilly, R. E., Flick, R. E., & Gutierrez, R. (2011). Short-term retreat statistics of a slowly eroding coastal cliff. *Natural Hazards and Earth System Sciences*, *11*(1), 205–217. https://doi.org/10.5194/nhess-11-205-2011

Young, A. P., Guza, R. T., Flick, R. E., O'Reilly, W. C., & Gutierrez, R. (2009). Rain, waves, and short-term seacliff evolution. *Marine Geology*, *267*, 1–7.

Young, A. P., Olsen, M. L., Driscoll, N., Flick, R. E., Gutierrez, R., Guza, R. T., et al. (2010). Comparison of airborne and terrestrial lidar estimates of seacliff erosion in Southern California. *Photogrammetric Engineering & Remote Sensing*, *76*(4), 421–427. https://doi.org/10.14358/PERS.76.4.421

Zedler, J. B. (2010). How frequent storms affect wetland vegetation: A preview of climate-change impacts. *Frontiers in Ecology and the Environment*, *8*(10), 540–547. https://doi.org/10.1890/090109

Zetler, B. D., & Flick, R. E. (1985). Predicted extreme high tides for mixed-tide regimes. *Journal of Physical Oceanography*, *15*(3), 357–359. https://doi.org/10.1175/1520-0485(1985)015<0357:PEHTFM>2.0.CO;2